JOURNAL OF AIRCRAFT
Vol. 34, No. 4, July–August 1997

Multiple Control Surface Utilization in Active Aeroelastic Wing Technology

G. Andersen,* E. Forster,† and R. Kolonay‡
U.S. Air Force Wright Laboratory, Wright–Patterson Air Force Base, Ohio 45433
and
F. Eastep§
University of Dayton, Dayton, Ohio 45469

This study investigates the use of multiple control surfaces to effect roll trim of aircraft. Analytic models of a rectangular wing and a fighter aircraft are used as examples for steady aeroelastic and antisymmetric trim analyses. The finite element method is used to calculate structural deformations caused by steady aerodynamic input forces, which are generated by a linear panel method. Values of control surface effectiveness, calculated from the flexible rolling moment stability derivatives, are used to determine which control surfaces are most effective in achieving a desired roll maneuver. The roll trim equation of motion is solved for multiple control surface deflections using an iterative technique that minimizes the control effort to achieve a specified roll rate. Roll trim utilizing multiple control surfaces, including leading-edge surfaces, is examined over a range of dynamic pressures. Aircraft models with reduced wing stiffness are investigated to determine if roll performance requirements can be achieved through the use of multiple control surfaces. The results of utilizing multiple control surfaces on flexible wings are examined to determine if weight savings can be achieved while maintaining a desired level of roll performance.

Nomenclature

A = normal velocity influence coefficient matrix
A_f = aerodynamic stiffness matrix caused by structural displacements
A_r = aerodynamic stiffness matrix caused by control surface deflections
b = reference span
C_M = rolling moment coefficient
C_{M_p} = derivative of rolling moment coefficient with respect to roll rate
$\boldsymbol{C}_{M_\delta}$ = $\{C_{M_{\delta 1}}, C_{M_{\delta 2}}, C_{M_{\delta 3}}, \ldots C_{M_{\delta n}}\}^T$, vector of derivatives of rolling moment coefficient with respect to control surface deflection
$C_{M_{\delta i}}$ = derivative of rolling moment coefficient with respect to a control surface deflection
E = elastic modulus
G = shear modulus
I = area moment of inertia
I_{roll} = moment of inertia about roll axis
J = torsional rigidity
K = structural stiffness matrix
M = structural mass matrix
n = number of control surfaces
p = roll rate
$\dot{p}$ = roll acceleration
q = dynamic pressure
S = aerodynamic surface reference area
U = induced velocity matrix
V_0 = freestream velocity
$\boldsymbol{x}$ = nodal displacement vector
$\ddot{\boldsymbol{x}}$ = nodal acceleration vector
$\boldsymbol{\gamma}$ = vortex panel singularity strength vector
$\boldsymbol{\delta}$ = $\{\delta_1, \delta_2, \delta_3, \ldots \delta_n\}^T$, control surface deflection vector
$\boldsymbol{\varepsilon}$ = $\{\varepsilon_1, \varepsilon_2, \varepsilon_3, \ldots \varepsilon_n\}^T$, control surface effectiveness vector
ε_i = control surface effectiveness
$\boldsymbol{\omega}$ = induced normal velocity vector

Presented as Paper 96-1443 at the AIAA/ASME/ASCE/AHS/ASC 37th Structures, Structural Dynamics, and Materials Conference, Salt Lake City, UT, April 15–17, 1996; received Oct. 5, 1996; revision received March 28, 1997; accepted for publication March 28, 1997.

*Aerospace Engineer, Flight Dynamics Directorate, and U.S. Air Force Lieutenant.
†Aerospace Engineer, Flight Dynamics Directorate.
‡Aerospace Engineer, Flight Dynamics Directorate. Member AIAA.
§Professor, Aerospace Engineering. Associate Fellow AIAA.

Introduction

ROLLING maneuvers for aircraft are conventionally performed by deflecting the trailing-edge control surfaces of the wings antisymmetrically, thereby increasing lift on one wing while decreasing lift on the other. During a conventional rolling maneuver, the chordwise moment caused by the aerodynamic forces generated by the deflected control surface on a flexible wing reduces the roll rate of the aircraft. As dynamic pressure increases, a point is reached where roll reversal occurs. Design engineers have traditionally added structure to stiffen the wing to avoid roll reversal in the operational flight envelope of the aircraft. While optimization techniques can minimize the weight penalty associated with increasing the structural stiffness, they do not directly take into account the effects of wing flexibility on rolling maneuver performance.

Active aeroelastic wing (AAW) technology is among recent endeavors to address this issue. The AAW concept integrates aerodynamics, controls, and structures disciplines to maximize aircraft performance.[1] Traditional design methods view structural flexibility as undesirable because it can result in reduction of control effectiveness.[2] Aeroelastic flexibility is utilized by AAW technology by employing multiple leading- and trailing-edge control surfaces as tabs that twist the wing.[3] When applying this concept, smaller control surface deflections are required for rolling maneuvers, and the more flexible wing actually twists less than a conventionally designed wing. Benefits of this technology include maximization of maneuver

control power for rolling and pitching, minimization of structural loads, and minimization of drag.[4] These advantages can be realized on a wing that is more flexible than a conventional design, which offers the potential of weight savings.

The goal of this effort was to explore the simultaneous use of multiple control surfaces in the application of AAW technology. Specifically, the capabilities of multiple control surfaces to effect roll maneuver trim of an aircraft with flexible wings were examined. Steady aeroelastic studies were performed on two models. The first was an unswept rectangular wing with a beam modeling the wing structural stiffness. The second was a model of a complete fighter aircraft, with beams modeling the major structural components. General trends involving effectiveness of the control surfaces with variation in dynamic pressure were generated to establish a foundation for multiple control surface scheduling. Reduction of the wing stiffness of the aircraft models was then used to establish whether roll performance requirements could be met using multiple control surfaces on a flexible wing. Finally, these studies were used to illustrate the increased roll maneuver control power generated through implementation of AAW technology.

Background

Analytic Tools

The automated structural optimization system (ASTROS) was used for all analyses in this effort. ASTROS is a multidisciplinary design tool capable of incorporating static, dynamic, and aerodynamic disciplines in the analysis and optimization of finite element models.[5] Steady aeroelastic trim analyses can be performed in which the roll rate and control surface deflections are included. In previous versions of ASTROS, when trimming for roll, only one variable could be free for solution of the trim equation; therefore, at the most, one control surface deflection could be utilized as a variable for antisymmetric trim analyses.

The inability of previous versions of ASTROS to utilize multiple control surfaces for trim was addressed by Northrop Grumman, under contract with the U.S. Air Force. Through that effort, an enhanced trim module for ASTROS called the adaptive multi-dimensional integrated controls (AMICS) module was created. AMICS incorporates a subset of the generic control law for conceptual and preliminary design.[6] This algorithm automates control surface scheduling based on aircraft stability derivatives for trim and transient maneuvering. In general, any number of control surfaces may be included in the analysis. A unique solution for an arbitrary number of control surface deflections is achieved through an iterative technique, during which the algorithm minimizes the control effort to achieve a desired maneuver performance.

Aeroelastic Analysis

All analyses were performed within the ASTROS environment, which uses a linear panel method to determine the aerodynamic loads, and the finite element method to determine the structural response. Standard surface and beam-splining techniques were applied to transfer the aerodynamic loads from the aerodynamic grid points to the structural grid points. The program's static aeroelastic analysis discipline was employed to generate stability derivatives as well as to solve the roll equation of motion and the roll trim equation.

The unified subsonic and supersonic aerodynamic analysis (USSAERO) algorithm is utilized in ASTROS (Ref. 7) for the computation of aerodynamic loads on the aircraft structure. For a lifting surface, this approach uses a superposition of vortex singularities applied to a discrete number of aerodynamic panels to determine the pressure distribution about the surface. The basic equation is

$$A\boldsymbol{\gamma} = \boldsymbol{\omega} \tag{1}$$

from which the panel vortex singularity strengths are calculated. Velocity components are then computed and the pressure coefficient at each of the panels is obtained. The pressure coefficients are converted to forces, which, in turn, yield the rigid aerodynamic loads. The aerodynamic influence coefficient matrix is generated to calculate the incremental loads caused by structural deformations. This matrix calculation is given by

$$\mathrm{AIC} = -4SUA^{-1} \tag{2}$$

where AIC is the aerodynamic influence coefficient matrix.

The steady aeroelastic features in ASTROS provide the capability to analyze linear structures in the presence of steady aerodynamic loading. The equation of motion is

$$M\ddot{\boldsymbol{x}} + (K - A_f)\boldsymbol{x} = A_r\delta \tag{3}$$

where A_f and A_r are generated from AIC. The stability derivatives, or sensitivities of C_M, with respect to the roll rate and control surface deflections, are calculated from the aerodynamic stiffness matrices. These derivatives can be used to quantify the ability of a particular control surface to generate rolling moments. Control surface effectiveness is defined as the ratio of a flexible control surface stability derivative to the flexible roll damping stability derivative. For an arbitrary number of control surfaces, the effectiveness values are given by

$$\varepsilon_i = -\frac{C_{M_{\delta i}}}{C_{M_p}}, \qquad i = 1, \ldots, n \tag{4}$$

Control surface reversal occurs when the control surface effectiveness becomes negative. In the examples studied in this effort, effectiveness values were determined as a function of dynamic pressure, thereby indicating the usefulness of each control surface over a range of flight conditions.

Another analysis technique was to determine the control surface deflections required to achieve a desired roll rate. The steady trim equation for roll is

$$qSb[\boldsymbol{C}_{M_\delta}^T\delta + C_{M_p}(pb/2V_0)] = I_{\mathrm{roll}}p \tag{5}$$

and may be solved within ASTROS for roll rate, roll acceleration, or control surface deflection. The problems explored in this study were simplified by the assumption of constant roll rate, or $p = 0$. Utilizing this assumption and employing the definition of control surface effectiveness, the trim equation may be recast as

$$\boldsymbol{\varepsilon}^T\boldsymbol{\delta} = pb/2V_0 \tag{6}$$

By employing Eq. (6), trends may be generated showing the disadvantage of using a single trailing-edge control surface on a flexible wing to generate roll power. By specifying a control surface deflection and solving for roll rate over a range of dynamic pressures, the loss in ability of an aileron to produce a desired roll rate can be demonstrated. Figure 1 illustrates this behavior. Roll reversal is seen where the roll rate changes sign from positive to negative for a given control surface deflection. Another means of quantifying this deficiency is by specifying a desired roll rate and solving for the deflection necessary to achieve trim. The asymptotic behavior of the aileron deflection as roll reversal is approached is illustrated in Fig. 2.

For a single control surface, the solution of Eq. (6) is trivial. For multiple control surfaces, however, an infinite number of solutions exist. The AMICS enhanced trim module provides the capability to determine a unique solution. The method of solving the trim equation for multiple control surfaces is an iterative scheme based on a minimum control energy criteria in which the effectiveness of each control surface is considered. In effect, this procedure minimizes the overall control surface actuator command signals, enabling a roll maneuver to

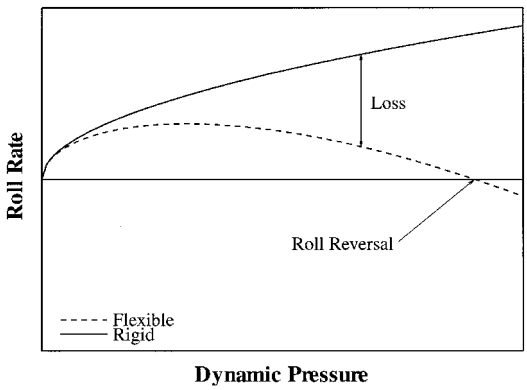

Fig. 1 Flexible and rigid roll rates for specified aileron deflection.

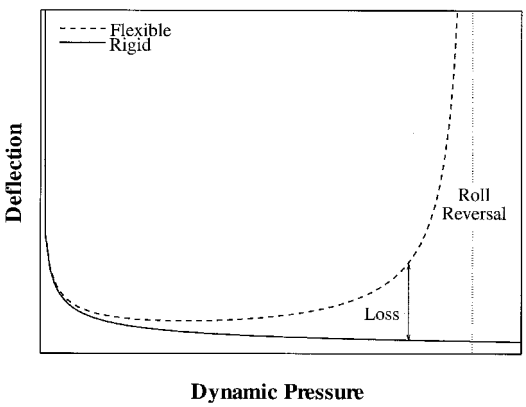

Fig. 2 Flexible and rigid aileron deflections for specified roll rate.

be performed using the minimum amount of control surface deflections.

Examples

Rectangular Wing

A rectangular wing model[8] was first used to demonstrate the general advantages of employing AAW technology. The structure was modeled as a beam divided into 10 finite beam elements, capable of supporting bending and torsional loads. The beam was positioned to place the elastic axis of the wing at one-third chord from the leading edge. Material properties were that of aluminum, with $E = 1.498 \times 10^9$ lbf/ft^2 and 6 = 5.616×10^8 lbf/ft^2. Structural properties of the beam elements were constant across the span, with $I = 1.579 \times 10^{-2}$ ft^4 and $J = 4.256 \times 10^{-3}$ ft^4. The unswept aerodynamic planform was modeled as a flat plate and contained a single leading-edge and a single trailing-edge control surface. Both surfaces were a constant 25% chord in width and spanned the outboard half of the wing. The chord and semispan of the wing were 6 and 20 ft, respectively. The structural and aerodynamic model is illustrated in Fig. 3.

All studies were performed at a Mach number of 0.8 while varying the dynamic pressure from 10 to 500 psf. To determine the effects of reduced structural stiffness, the wing was analyzed as its torsional stiffness was reduced from the original stiffness to 75% and then 50% of the original value. Because of the simple geometry of the wing, the bending and torsional structural responses of the wing were uncoupled; therefore, the bending stiffness of the wing was not varied since the aeroelastic behavior of interest consisted purely of torsional effects.

Analysis of the aeroelastic behavior of the wing began with an examination of the effectiveness of the control surfaces at the various stiffnesses. Figure 4 illustrates these results. The trailing-edge surface exhibited behavior typical of an aileron;

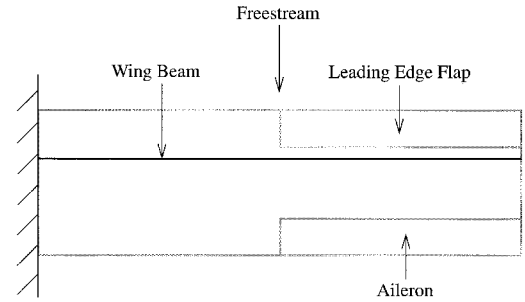

Fig. 3 Rectangular wing finite element and aerodynamic models.

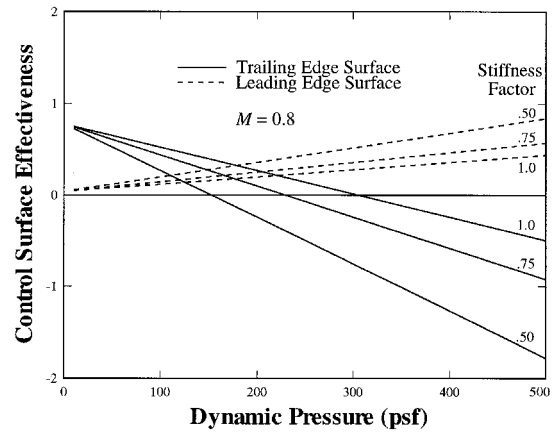

Fig. 4 Control surface effectiveness at various stiffnesses.

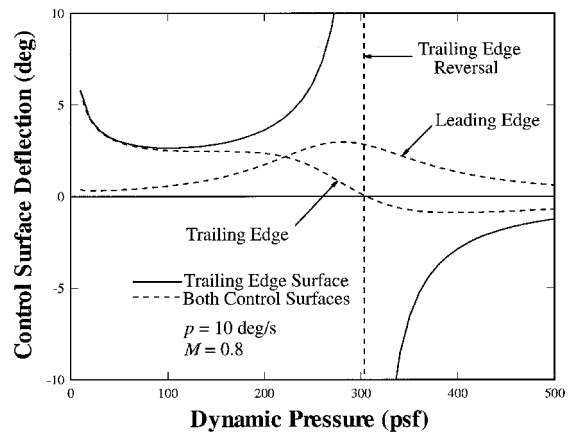

Fig. 5 Control surface deflections for trim.

control effectiveness decreased and passed through zero as the dynamic pressure increased. Further, the trailing-edge effectiveness decreased with a reduction in stiffness, which resulted in reduced reversal speeds as the wing became more flexible. In contrast, the leading-edge surface effectiveness increased as dynamic pressure increased and stiffness decreased. Unlike the trailing-edge surface, the leading-edge surface effectiveness was at all times positive, indicating the usefulness of leading-edge control surfaces over a wide range of dynamic pressures.

The advantages of utilizing leading-edge roll effectors are again shown in Fig. 5. Here, two control surface actuation schemes were employed to achieve a desired roll rate. The first considered using only the trailing-edge surface to provide the necessary roll power. The second used a combination of leading- and trailing-edge surface deflections. When only the trailing-edge surface was employed, the deflections became very large as the reversal dynamic pressure was approached. At the reversal point, the trailing-edge surface alone could not generate the desired roll rate.

The use of both control surfaces resulted in more efficient use of control surface deflections. At low dynamic pressures, the trailing edge was the more effective surface and provided the majority of the roll power. However, as the reversal point was approached and the trailing-surface effectiveness tended to zero, the leading-edge surface became dominant until, at the reversal point, the trailing-edge surface was neutralized while the leading-edge surface generated the entirety of the roll power. Beyond reversal, the trailing-edge surface again became effective and produced a portion of the roll power, even though the surface was deflected in a direction opposite of the prereversal deflection. This demonstrates the usefulness of a trailing-edge control surface as a roll effector beyond control surface reversal.

The benefits of using leading- and trailing-edge control surfaces simultaneously are further illustrated in Fig. 6, where the control surface deflections needed to achieve a specified roll rate are shown. Assuming a 5-deg limit on the deflection angles, roll rates of up to 30 deg/s were obtained for all but the lowest dynamic pressures. The plot illustrates that the reversal point remained a critical factor in achieving a desired roll rate. Near the reversal point, the trailing-edge surface effectiveness approached zero and the leading-edge surface alone was required to produce the desired roll rate. Consequently, the reversal dynamic pressure required the largest control surface deflections. These modest deflections, however, produced a significant roll rate at the reversal dynamic pressure; in contrast, when only the trailing-edge surface was used, the deflections tended to infinity.

Finally, the effects of reduced wing stiffness on required control surface deflections were examined. Figure 7 shows the deflections of the control surfaces needed to achieve the target roll rate of 10 deg/s as the wing stiffness was reduced to one-half of the original value. For this particular wing geometry and control surface configuration, little additional control effort was needed to achieve the same roll rate. A 50% reduction in the stiffness required only slightly more than a single deg increase in the deflection of the leading-edge surface, and less than one-half deg for the trailing edge, indicating little sensitivity of required control effort to large variations in the structural stiffness of the wing.

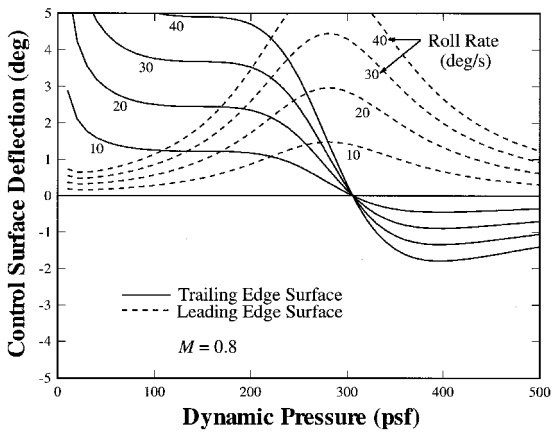

Fig. 6 Control surface deflections for trim at various roll rates.

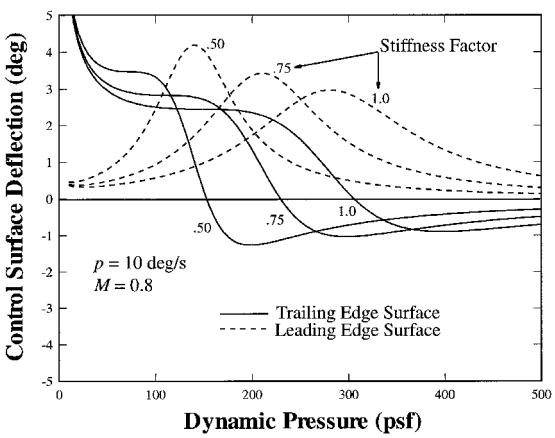

Fig. 7 Control surface deflections for trim at various stiffnesses.

The results obtained from the analysis of the unswept rectangular wing emphasize the effectiveness of utilizing a leading-edge control surface to augment roll performance over a large range of dynamic pressures, particularly near the reversal point. They also demonstrate that a trailing-edge surface can be used as a roll effector beyond reversal. Furthermore, since this example showed that roll performance can be sustained with more flexible wings through the use of leading- and trailing-edge control surfaces, and because reduced wing stiffness suggests a lower structural mass, these results imply that wing structural weight savings can be realized through implementation of AAW technology.

Fighter Aircraft

This example utilized a half model of a typical fighter aircraft (Fig. 8), where the fuselage, wing, horizontal tail, and vertical stabilator were modeled as beams. The main wing beam was attached to the fuselage beam by rigid bar elements. The control surfaces were also modeled as beams, with rigid bars connecting the hinge line and spring-modeled actuators. The fuselage beam ran along the centerline from the cockpit to the horizontal tail. The wing, stabilator, and control surface beams were located along their respective elastic axes. The wing and stabilator beams both ran approximately along the 40% chord of their respective aerodynamic surfaces. Although the model is representative of the geometry of the F/A-18 aircraft,[9] the structural and material properties do not necessarily correspond to those of the actual vehicle; consequently, results generated from this model should be considered qualitative in nature.

The wing and horizontal stabilator were modeled as aerodynamic surfaces and extended to the aircraft centerline. The wing had a semispan of 225 in., with a root chord of 190 in., and a tip chord of 65 in. The wing leading edge was swept aft at 27 deg. The stabilator had a semispan of 130 in., with a root chord of 120 in., and a tip chord of 45 in. The stabilator leading edge was swept aft at 47 deg. The leading-edge hinge line was located at the 19% chord. The leading-edge inboard flap began at a span location of 54 in. and extended to the 165-in. span station while the leading-edge outboard flap continued from the 165-in. span station to the wing tip. The trailing-edge hinge line was located at the 68% chord. The trailing-edge flap began at a span location of 42 in. and extended to the 154-in. span station. The aileron continued from the 154-in. span station to the wing tip.

The fighter aircraft was first analyzed to establish static aeroelastic behavior trends. At Mach 0.9, the model was analyzed for roll trim at a constant roll rate of 90 deg/s over a range of dynamic pressures. The flexible stability derivatives

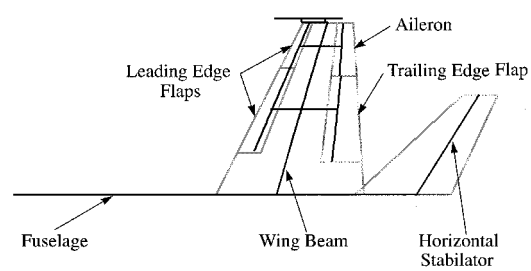

Fig. 8 Sketch of fighter aircraft finite element and aerodynamic models.

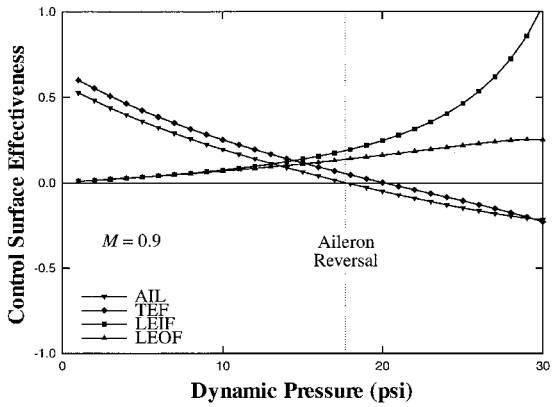

Fig. 9 Control surface effectiveness.

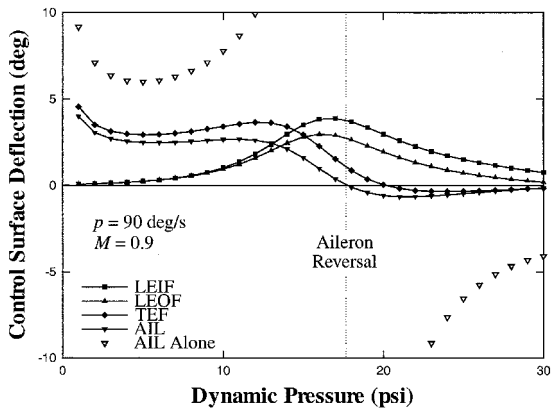

Fig. 10 Control surface deflections for trim.

established the effectiveness of the control surfaces. The control surface effectiveness is illustrated in Fig. 9 for the leading-edge inboard flap (LEIF), leading-edge outboard flap (LEOF), trailing-edge flap (TEF), and aileron (AIL). It is worth noting that the trailing-edge flap and leading-edge inboard control surfaces generally had higher effectiveness than their outboard counterparts. This is because the inboard surfaces had much larger areas than the outboard surfaces. Also evident is that with increasing dynamic pressure there was increasing effectiveness of the leading-edge control surfaces and decreasing effectiveness of the trailing-edge control surfaces. The control surface effectiveness of the aileron became negative at 18 psi, indicating that roll reversal had occurred. The trailing-edge flap reversal occurred at 20 psi.

Control surface deflections required for trim of the aircraft are illustrated in Fig. 10. for both a standard single aileron as well as simultaneous use of all four control surfaces. Trim employing the aileron alone generated an asymptotic trend about the roll reversal dynamic pressure. From 6 to 10 deg of deflection of the aileron were needed for dynamic pressures up to 12 psi, and an increasingly large deflection was needed as aileron reversal was approached. Above the reversal point, the deflection required for trim was negative and decreased from large values near the reversal point to around -5 deg at high dynamic pressures. When trim was achieved by simultaneously using leading- and trailing-edge control surfaces, required deflection magnitudes were no greater than 5 deg for any one surface. The largest deflection occurred at the leading-edge inboard flap at a dynamic pressure slightly less than that of aileron reversal. At higher dynamic pressures the deflections were considerably smaller.

The deflections of the control surfaces appear to be dependent upon the relative values of control surface effectiveness. It is apparent that where the trailing-edge flap deflection was larger than that of the aileron deflection, the trailing-edge flap control surface effectiveness was greater than that of the aileron effectiveness. The leading-edge inboard flap deflection was also higher than that of the leading-edge outboard flap. The leading-edge flap deflection became greater than the trailing-edge flap deflection at the same dynamic pressure at which the control surface effectiveness of the leading-edge flap became greater than that of the trailing-edge flap. Also notable is that the aileron and trailing-edge flap trimmed deflections were zero at the dynamic pressure at which control surface effectiveness values were zero, thereby taking advantage of the more effective control surfaces to trim the aircraft.

The next analysis of this model was intended to show the increased roll power of an aircraft with reduced wing stiffness. Because of the spanwise bending effect on freestream angle of attack of a swept wing, the bending as well as the torsional stiffness was reduced. Therefore, the reduced stiffness aircraft was modeled with 50% wing torsional (GJ) and 50% bending stiffness (EI) of the original aircraft. For comparison, the model was again analyzed for roll trim at Mach 0.9, at a constant roll rate of 90 deg/s. The values of control surface effectiveness for all four surfaces are illustrated in Fig. 11. The trends are similar to those of the original stiffness model. The most noticeable difference is apparent at high dynamic pressures in which control surface effectiveness values for the leading-edge flaps for the reduced stiffness model were higher than that of the original stiffness model. Similarly, for high dynamic pressures, the trailing-edge control surfaces had a lower control surface effectiveness than the original stiffness model. Roll reversal for the aileron occurred at a lower dynamic pressure of 12 psi.

Control surface deflections to achieve trim for the reduced stiffness model are shown in Fig. 12. Again, the single aileron deflections as well as the multiple control surface deflections are illustrated. The trim capability of the single aileron was

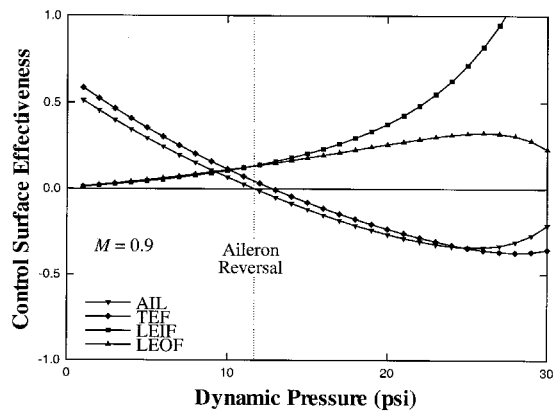

Fig. 11 Control surface effectiveness for reduced stiffness model.

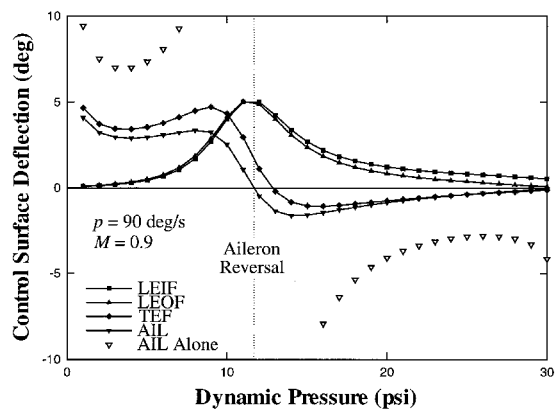

Fig. 12 Control surface deflections for trim for reduced stiffness model.

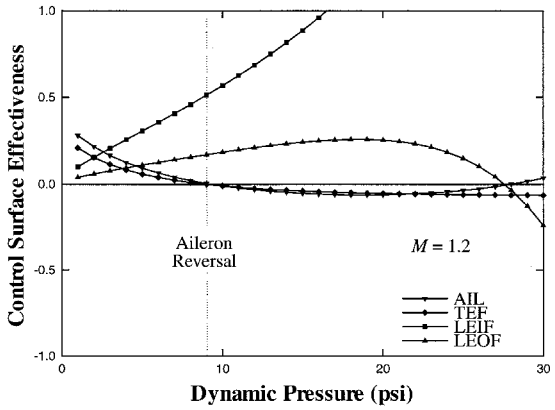

Fig. 13 Control surface effectiveness for reduced stiffness model.

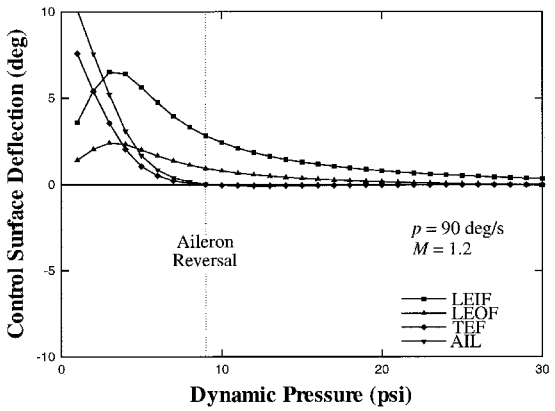

Fig. 14 Control surface deflections for trim for reduced stiffness model.

substantially diminished in the reduced stiffness model. The aileron was only able to produce the rolling maneuver with deflections of 7–10 deg up to a dynamic pressure of 7 psi. The multiple control surfaces, however, were easily able to achieve trim throughout the entire range of dynamic pressures. The largest deflections occurred at the reversal point, though they were only slightly larger than the deflections required of the original stiffness model. The deflection trends for the reduced stiffness model are similar to those of the original stiffness model. The most noticeable benefit of the reduced stiffness wing was the resulting small control surface deflections required at high post-reversal dynamic pressures.

To further illustrate the benefits of multiple control surface utilization to achieve trim, the reduced stiffness model was analyzed using supersonic aerodynamics at Mach 1.2 at a constant roll rate of 90 deg/s. The control surface effectiveness values for all four surfaces are shown in Fig. 13. The notable differences in the control surface effectiveness behavior were because of the change in the aerodynamic center location when supersonic aerodynamics were used. The leading-edge surfaces had a generally higher control surface effectiveness than in the subsonic case, while the trailing-edge control surfaces had lower effectiveness. The leading-edge inboard control surface was the most effective. The aileron had a higher effectiveness than the trailing-edge flap, and both surfaces reversed at a dynamic pressure of 9 psi. After reversal, the trailing-edge flap and aileron were generally ineffective.

The trim results for the multiple control surfaces are illustrated in Fig. 14. The aileron and trailing-edge control surfaces were deflected from 5 to 10 deg up to a dynamic pressure of 3 psi. At this point the leading-edge surfaces became more effective. The leading-edge inboard flap reached a maximum deflection of 7 deg between 4–5 psi, well before aileron reversal occurred. Beyond reversal, the flap deflections required became quite small, primarily because of the effectiveness of the LEIF.

Analysis of a typical fighter aircraft indicates the advantage of using multiple control surfaces in achieving roll trim at both subsonic and supersonic flight conditions. The usefulness of leading-edge control surfaces is particularly evident at high dynamic pressures. Roll performance is maintained for reduced stiffness wings, with little additional control power needed.

Conclusions

The examination of a rectangular wing and fighter aircraft model shows implementation of AAW technology to be a viable design methodology. Utilization of leading-edge control surfaces can be effectively employed to effect aircraft trim across a wide range of dynamic pressures. Roll trim can be achieved using multiple control surfaces with smaller deflections than with a single surface. Examination of reduced stiffness models illustrates that wing flexibility is beneficial when utilizing AAW technology to effect roll maneuver trim. Reduced wing stiffness requirements translate to aircraft weight savings, thereby establishing the benefits of this alternate design approach in which the roll performance of aircraft can be enhanced by incorporating AAW concepts in the early stages of aircraft design.

Acknowledgments

The authors acknowledge the support received from the Air Force Office of Scientific Research under the University Residency Research Program during this investigation.

References

[1]Miller, G. D., "Active Flexible Wing (AFW) Technology," Air Force Wright Aeronautical Lab., TR-87-3096, Feb. 1988.

[2]Miller, G. D., "An Active Wing Multi-Disciplinary Design Optimization Method," *AIAA 5th Symposium on Multidisciplinary Analysis and Optimization* (Panama City, FL), AIAA, Washington, DC, 1994, pp. 1388–1394.

[3]Pendleton, E., Lee, M., and Wasserman L., "Application of AFW Technology to the Agile Falcon," *Journal of Aircraft*, Vol. 29, No. 3, 1992, pp. 444–451.

[4]Yurkovich, R., "Optimum Wing Shape for an AFW," *AIAA 36th Structures, Structural Dynamics, and Materials Conference* (New Orleans, LA), AIAA, Washington, DC, 1995, pp. 520–530.

[5]Neill, D. J., and Herendeen, D. L., "Automated Structural Optimization System (ASTROS)," *Users Manual*, Vol. 1, Air Force Wright Aeronautical Labs., TR-93-3025, March 1993.

[6]Ausman, J. D., "Adaptive Multi-Dimensional Integrated Control (AMICS) ASTROS Add-On Documentation," Air Force Wright Aeronautical Labs. Contract F33615-93-C3615, Interim Rept., Nov. 1995.

[7]Johnson, E. H., and Venkayya, V. B., "Automated Structural Optimization System (ASTROS)," *Theoretical Manual*, Vol. 1, Air Force Wright Aeronautical Labs., TR-88-3028, Dec. 1988.

[8]Eastep, F. E., and Olsen, J. J., "Transonic Flutter Analysis of a Rectangular Wing with Conventional Airfoil Sections," *AIAA Journal*, Vol. 18, No. 10, 1980, pp. 1159–1164.

[9]Grimes, P. J., "F/A-18 Airframe Compliance and Ground Vibration Data Report," McDonnell Aircraft Co., MDC A5773, Addendum B, Jan. 1982.